Effective Equalization for Overlapped Chirp-based Communications Systems

Thuy M. Pham, André N. Barreto, Sayed Hossein Dokhanchi, Gerhard Fettweis
Barkhausen Institut, Dresden, Germany
{minhthuy.pham, andre.nollbarreto, hossein.dokhanchi, gerhard.fettweis}@barkhauseninstitut.org

***Abstract*—In this paper, we consider different equalization techniques for chirp-based communications systems. Although chirps are more commonly used for radar systems, several studies show their potential for either low-rate communication or for high spectral efficiency using an overlapping technique. However, previous literature has dealt only with additive white Gaussian noise (AWGN) channels. In this paper, we investigate the overlapped chirps under multipath channel models. More specifically, we model the overlapped chirp-based communication system and then reformulate the receive signals to which common linear and non-linear equalizers are applicable. For the purpose of benchmarking, we demonstrate the effectiveness of those equalizers in a realistic 5G tapped delay line (TDL) channel model. Our simulation results show that, with proper equalization, overlapped chirps can also operate under multipath channels, and that non-linear equalization methods outperform linear ones.**

***Index Terms*—overlapping, chirp, equalization, spectral efficiency, multipath.**

I. Introduction

Frequency-modulated continuous wave (FMCW) signals, also known as chirps, play an important role in radar systems, especially for automotive applications, specifically due to the possibility of low-complexity hardware implementations and of their robustness against channel impairments. Beyond their use for radar detection, some studies have also considered chirp for communications [1]–[5]. Recently, there is renewed interest in using chirps for communications, due to their potential applications in joint communications and sensing (JC&S), which is expected as one of the key features of beyond 5G systems [6]–[8].

Chirps can be transmitted either as non-overlapping or overlapped signals. For example, non-overlapping frequency-shift keying (FSK)-modulated chirps can be used for both radar detection and low-spectral-efficiency communications [9]. On the other hand, overlapped chirps can increase the spectral efficiency significantly. Overlapped chirps can be generated digitally using a Fresnel transform, in the orthogonal chirp-division multiplexing (OCDM) approach [5], [10], but also in the time domain, by reducing the interval between consecutive modulated chirps [4], [11], which offers the possibility of lower-complexity hardware. Different from the binary orthogonal keying (BOK) approach, which employs both up-chirp and down-chirp for communications [2], [3], a linear modulation scheme can be used, in which each chirp is modulated in phase and/or amplitude for communications [11]. However, whereas different chirps in OCDM are orthogonal, the same cannot be held for time-shifted overlapped chirps, except for very specific conditions [11]. In [4], the authors derive a bit error rate (BER) formula for an infinite number of overlapped chirps at a low spectral-efficiency regime, but do not consider methods to compensate for the intersymbol interference (ISI) between chirps. In [11], the BER under a finite number of chirps was formulated together with extensive analysis of the intersymbol interference power for different spectral efficiency. In addition, the authors in [11] show that simple linear equalizers, such as zero-forcing (ZF) can be utilized to achieve the Nyquist signalling rate with sufficient low BER close to that of non-ISI one. However, the studies of both [4] and [11] are only limited to the ideal additive white Gaussian noise (AWGN) channel.

In this paper, we investigate the chirp-based communications in multipath channel, which is usually the case in practice. More importantly, we consider different equalization techniques to find a proper equalizer for this severe ISI condition. In particular, linear equalizers, such as ZF, may not provide sufficient performance improvement. Therefore, nonlinear equalizers are also investigated. In fact, the optimal performance can be achieved with a maximum likelihood (ML) equalizer, but it can be computationally prohibitive. Because of this drawback, here we also investigate fixed sphere decoder (FSD) and zero-forcing ordered successive interference cancellation (ZF-OSIC) [12]–[15], which can provide a good trade-off between complexity and performance.

Our main contributions include the following:

- To the best of the authors' knowledge, we are the first to work on equalization for overlapped chirps in a multipath channel model.
- We arrive at a simplified representation for equalization, considering the combination of the multipath channel and the inter-chirp interference.
- We apply different equalization techniques for the system of interest. More specifically, we study both linear and non-linear equalization methods to find the most appropriate ones.
- The effectiveness of the equalization is evaluated extensively by means of simulation. In addition, we have executed our simulations using a standard 5G multipath channel model [16], which has not been reported before.

In Section II we describe the system model and the equalization algorithms. We then present and analyze simulation

results in Section III and conclude the paper in Section IV.

Notation: Bold lower- and upper-case letters represent vectors and matrices, respectively. In addition, $a \in \mathbf{A}$ means a is an element of $\mathbf{A}$ whereas $\mathbf{A} \subseteq \mathbf{B}$ indicates that $\mathbf{A}$ is a subset of $\mathbf{B}$. $\circledast$ denotes the convolution and $\mathcal{O}()$ is a notation for the asymptotic complexity of algorithms. The floor function $\lfloor x \rfloor$ gives the greatest integer value less than or equal to x.

II. System Model and Equalization Techniques

A. System Model

Let $\mathcal{C}$ denote the complex constellation set of a modulation scheme. For instance, a $\mathcal{C}$ of an M-ary phase shift keying (M-PSK) or an M-quadrature amplitude modulation (M-QAM) will consist of M constellation points. A modulated chirp signal is defined as

$$u_k(t) = \vartheta_k s(t), \tag{1}$$

where $\vartheta_k \in \mathcal{C}$ represents the k-th data symbol, and

$$s(t) = \frac{1}{\tau_{\mathrm{d}}} e^{j\pi\mu t^2}, \quad |t| \leq \frac{\tau_{\mathrm{d}}}{2} \tag{2}$$

is a complex baseband chirp signal. Note that $\mu = B/\tau_{\mathrm{d}}$ is the chirp slope, with B and τ_{d} the chirp bandwidth and duration, respectively. As a result, we can express a communications signal consisting of κ overlapped chirps as follows

$$x(t) = \sum_{k=0}^{(\kappa-1)} u_k(t - k\tau), \tag{3}$$

where τ is the delay between consecutive chirps.

Assuming perfect synchronization at the communication receiver, we obtain

$$y(t) = x(t) \circledast h_c(t) \circledast h_m(t) + n(t), \tag{4}$$

where $h_c(t)$ and $h_m(t) = s^*(-t)$ represent the impulse response of the channel and matched filter, respectively, and $n(t) = w(t) \circledast h_m(t)$ is the zero-mean complex colored noise at the filter output, with $w(t)$ the white Gaussian noise component. In this paper, we assume that the channel impulse responses, i.e., $h_c(t)$ is perfectly known at the receiver.

Recall that the spectral efficiency $\eta = \frac{1}{\tau B}$ and thus τ plays an important role in increasing the spectral efficiency for a given bandwidth. In this paper, we are interested in the nontrivial case $\tau < \tau_d$. However, we need to compensate the severe ISI by proper equalization methods as shown in the following section.

B. Equalization Methods and Complexity

In what follows, we manipulate Eq. (4) to arrive at a generic form to which common equalizers and detectors are applicable. In particular, we rely on the following proposition to perform efficient detection.

Proposition 1. *Equation* (4) *can be equivalently expressed in the standard form:*

$$\mathbf{y} = \mathbf{H}\mathbf{x} + \mathbf{n} \tag{5}$$

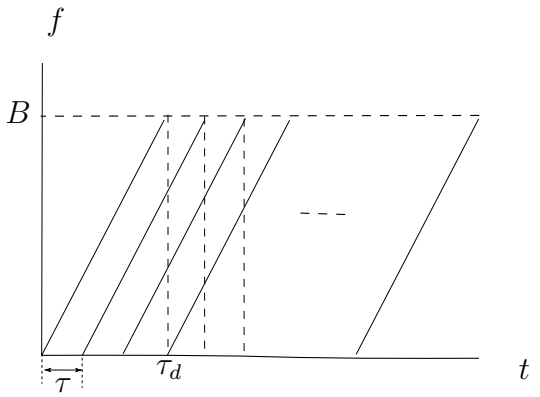

Fig. 1: Overlapped chirp-based communications signal

where $\mathbf{x} = [\vartheta_0, \vartheta_1, \ldots, \vartheta_{\kappa-1}]^T$, $\mathbf{y} = [y_0, y_1, \ldots, y_{\kappa-1}]^T$, $\mathbf{n} = [n_0, n_1, \ldots, n_{\kappa-1}]^T$, *and* $\mathbf{H}$ *is an effective channel matrix.*

Interested readers can refer to the Appendix for the detailed proof of Proposition 1. Note that the effective channel matrix $\mathbf{H}$ takes both channel impulse responses and ISI components into account and is generally *not a symmetric* matrix as the case of AWGN [11]. We also remark that the length of the received signal vector $\mathbf{y}$ can be larger than κ to account for the multipath delay spread. To simplify the analysis, we have however chosen to consider only κ samples at the output which can still preserve sufficient information of both multipath and ISI components while providing low-complexity matrix operations.

In [11], the authors showed that simple linear equalization methods, such as zero-forcing (ZF), can be sufficiently efficient for AWGN channels. We demonstrate shortly in the numerical results that this approach no longer works for the multipath channel model. Instead, we have to turn to nonlinear methods, which are more promising for the considered problem. More specifically, we consider the following non-linear equalizers and detectors.

1) Maximum likelihood (ML): We try to solve the following problem:

$$\hat{\mathbf{x}} = \underset{\mathbf{x} \in \mathcal{C}^\kappa}{\arg\min} ||\mathbf{y} - \mathbf{H}\mathbf{x}|| \tag{6}$$

where $\mathcal{C}^\kappa$ is the constellation set of the transmitted symbols. For our considered problem, the complexity of the detection is $\mathcal{O}(M^\kappa)$, which becomes excessively high when we increase the number of symbols or the constellation size.

2) Fixed sphere decoder (FSD): Different from ML, which searches over the whole constellation, FSD assigns a fixed number of candidates per level which is generally less than or equal to M [14], [15]. Note that a level corresponds to an order of the symbol in the current context. Thus, only a subset $\mathcal{S} \subseteq \mathcal{C}$ will be searched and the complexity of the decoder is fixed. More importantly,

TABLE I: Common simulation parameters

Parameters	Value
Channel model	5G TDL
Mode	A
RMS delay	90 ns
Tx/Rx antennas	1/1
Chirp duration	1 μs
Channel realizations	12000

we can choose the number of candidates irrespective of the noise power.
For simplicity, we consider the first L levels will perform ML search and the rest will search over one candidate. In other words, the complexity of this approach is $\mathcal{O}(M^L)$. It is worth noting that the complexity of FSD is equal to that of ML when $L = \kappa$.

3) Zero-forcing ordered successive interference cancellation (ZF-OSIC): This approach has lower complexity in comparison with ML and can be referred to as sequential nulling and cancellation detection [12], [13]. The system first decodes and then cancels the strongest signal and then continues in this fashion for the remaining signals. The main operation contributing most to the complexity of the algorithm is the inverse of the channel ,i.e., $\mathcal{O}(\kappa^3)$. Thus, the overall complexity of this algorithm for our considered problem is $\mathcal{O}(\kappa^4)$.

As analyzed above, ML can achieve the optimal performance but suffers from high complexity, whereas FSD can trade off the performance and complexity. For further details of the equalization methods, we refer interested readers to [12]–[15]. The performance of these equalizers and detectors for our overlapped-chirp-based system under different spectral efficiency will be detailed in the Section III.

III. Numerical Results

In this section, we numerically evaluate the performance of the proposed approaches. We first give a concise summary of the channel model followed by the simulation results. It is worth noting that simulations were performed using our Python-based open-source link-level simulator, HermesPy [17].

We adopt the 5G tapped delay line (TDL) model for our simulations, which is one of realistic channel model standardized for 5G [16] studies. In the 5G TDL channel model, the first three modes (TDL-A, TDL-B, TDL-C) are designed for non-light-of-sight (NLOS) propagation, which is of our interest. Although the power delay profile and the number of taps are different for each mode, in all of them individual taps follow a Rayleigh distribution.

In the following, the chirp duration is fixed at 1 μs. For FSD, we consider the full constellation search for $L = \lfloor \kappa^{1/3} \rfloor$ symbols. In addition, we consider TDL-A for the majority of the simulations and the results are averaged over 12000 channel realizations. The common simulation parameters are summarized in Table I. Other parameters are specified for each setting, unless stated otherwise.

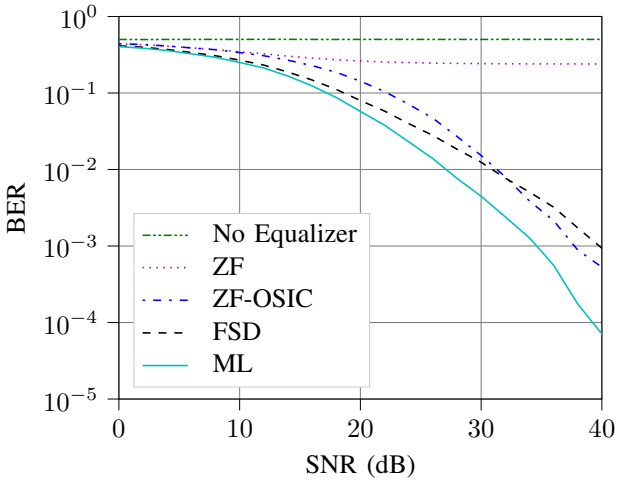

(a) $\eta = 0.2$

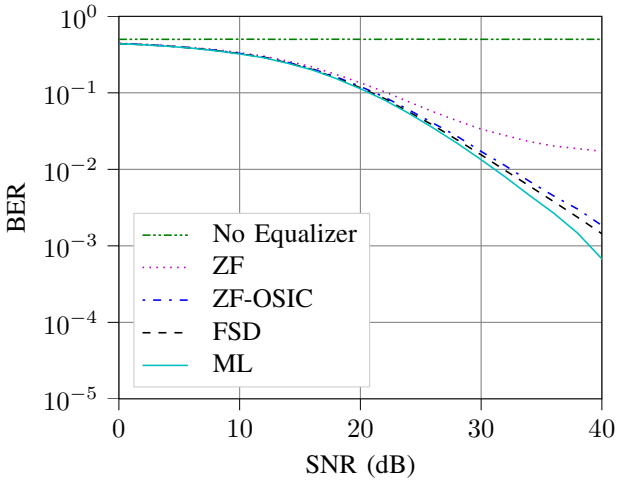

(b) $\eta = 1$

Fig. 2: Performance of linear and nonlinear equalizers under different spectral efficiency. Chirp duration $\tau_d = 1\mu$s and chirp bandwidth $B = 500$MHz.

In the first experiment, we set the bandwidth to 500 MHz and changes the chirp interval τ so that the spectral efficiency varies from $\eta = 0.2$ to the Nyquist signalling rate, i.e., $\eta = 1$. For the purpose of benchmarking all aforementioned equalization methods, we send a block of 10 binary phase-shift keying (BPSK)-modulated symbols so that high-complexity equalizers like ML can still generate the result without excessive cost. More importantly, the performance of ML can show the bounds for the remaining equalization methods. In fact, Fig. 2 has several implications. First, for the considered multipath system, we cannot decode a transmitted message properly without an equalizer. Second, linear equalization methods such as ZF do not work efficiently in a multipath environment. Note that the performance of ZF in higher overlapping rate is better than that of lower rate, possibly because the former corresponds to the case in which the noise is less amplified. Third, the optimal ML achieves the best performance followed

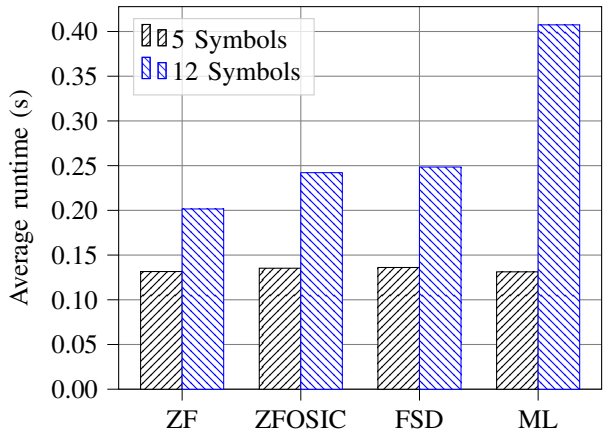

Fig. 3: Average runtime of different equalization methods.

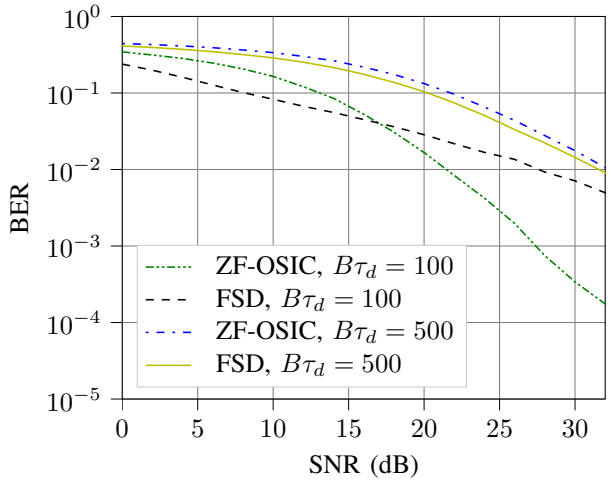

Fig. 4: Performance of nonlinear equalizers with varying values of time-bandwidth product.

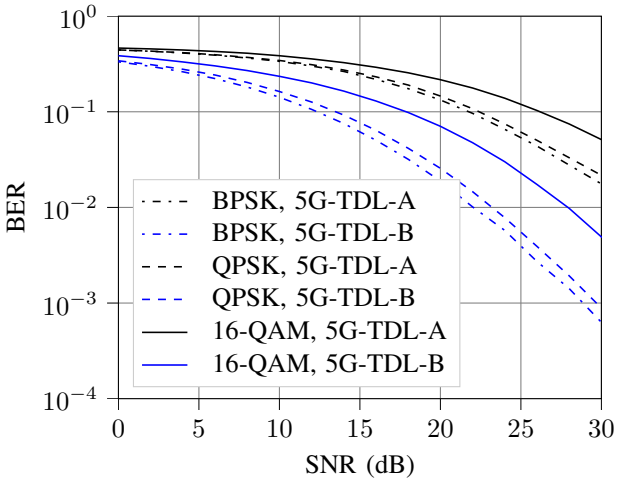

Fig. 5: Performance of ZF-OSIC under TDL-A and TDL-B channels.

by FSD and ZF-OSIC, as expected. Moreover, we can observe the performance degradation of these equalizers when the ISI becomes severe, e.g., at the Nyquist rate. Interestingly, nonlinear equalizers can still show acceptable performance.

Next, we consider the average runtime of a simulation with respect to the number of symbols. In particular, we vary the signal-to-noise ratio (SNR) from 0 to 48 dB with a stepsize of 2 dB and also change the number of symbols to record the runtime for the whole simulation. For a fair comparison, we executed the Python code on the same 64-bit desktop which supports 32 GB RAM and Intel Xeon Gold. In fact, the runtime, though including not only the complexity of the equalization or detection methods but also the complexity of the overall chirp-based systems, still relatively reflects the complexity of each equalization technique. Unsurprisingly, all methods have shown similar performance under a short block of data symbols, e.g., 5 symbols (c.f. Fig. 3). However, the difference will become significant when the number of symbols increases. For instance, for a block of 12 symbols, the runtime of ZF, ZF-OSIC, and FSD are still comparable while that of ML increases dramatically. As a consequence, FSD and ZF-OSIC can provide a good trade-off between those techniques, which is in line with what we discussed in the complexity analysis. It is however worth noting that if we increase the number of levels, i.e., L which perform ML search in FSD to improve the BER performance, its complexity will approach that of ML.

We now turn our attention to the effect of the time-bandwidth product on the performance of the chirp communications system. It is well-known that this value of radar systems is commonly large. In particular, we change the time-bandwidth product $B\tau_{\mathrm{d}}$ from 100 to 500, with BPSK at the Nyquist signalling rate. As can be seen from Fig. 4, the performance degrades with a higher value of time-bandwidth product. This phenomenon can stem from the severe effect of ISI when the main lobe of the chirps at matched-filter response is narrower.

In the last simulation, we study the performance of the equalization methods under different channel settings and modulation schemes, also at the Nyquist rate. Since we increase the block of symbols, e.g., 20, we choose ZF-OSIC for this simulation since it provides both good BER performance and low complexity, as shown in the preceding simulations. The BER curves of BPSK and QPSK after equalization show similar perfomance and are better than that of 16-QAM, which is consistent with the BER patterns of traditional modulation schemes. In TDL-A, the delay profile spreads over a larger range than under TDL-B, which possibly causes severe ISI under such high overlapping rate, i.e., Nyquist rate. Thus, its performance shows some degradation in comparison with the case of TDL-B (c.f. Fig. 5).

IV. Conclusion

We have studied the performance of communications systems using chirp pulses in multipath channels using 5G TDL channel model. More importantly, we have derived a

simple reformulation of the receive signal to which common equalization methods can be applied. Simulation results have shown that simple linear equalizers do not work efficiently but nonlinear ones do. Moreover, lower-complexity-than-ML techniques such as fixed sphere decoder (FSD) and zero-forcing ordered successive interference cancellation (ZF-OSIC) can provide a good trade-off between the performance and the complexity for our considered system.

ACKNOWLEDGEMENT

This work is financed by the Saxon State government out of the State budget approved by the Saxon State Parliament.

APPENDIX

PROOF OF TRANSFORMATION OF EFFECTIVE CHANNEL

Due to the commutativity property of the convolution, we can rewrite Eq. (4) as follows

$$y(t) = x(t) \circledast h_m(t) \circledast h_c(t) + n(t), \tag{7}$$

which in turn results in

$$y(t) = \sum_{k=0}^{(\kappa-1)} \vartheta_k r(t - k\tau_d) \circledast h_c(t) + n(t), \tag{8}$$

or equivalently,

$$y(t) = \sum_{k=0}^{(\kappa-1)} \vartheta_k h(t - k\tau_d) + n(t), \tag{9}$$

where $h(t) = r(t) \circledast h_c(t)$ and $r(t)$ is the output of the matched filter of a chirp signal.

In this paper, $h(t)$ represents both the transmit carrier, receive filter and the channel impulse response. Apart from pulses, those derivations are applicable to any other waveforms which are not necessarily limited to chirps. In case of the chirp signal considered in this paper, we have a closed-form formula for $r(t)$, which is commonly referred to as the chirp autocorrelation [2], [4] given by

$$r(t) = \frac{\sin\left(\pi B t (1 - \frac{|t|}{\tau_d})\right)}{\pi B t}, \quad |t| \leq \tau_d. \tag{10}$$

Each sample at the receiver will contain partial information of transmitted symbols and multipath components. As mentioned in Section II-B, we choose κ samples in the following analysis for the purpose of simplicity. After sampling at $t = i\tau, \quad i = 1 \ldots \kappa$ corresponding to κ transmitted symbols, the receive signal can be written in the discrete form as follows:

$$y_i = \sum_{k=0}^{(\kappa-1)} \vartheta_k h((i-k)\tau) + n_i, \tag{11}$$

or equivalently

$$y_i = \vartheta_0 h(i\tau) + \vartheta_1 h((i-1)\tau) + \vartheta_2 h((i-2)\tau) + \ldots + \vartheta_{\kappa-1} h((i-\kappa+1)\tau) + n_i. \tag{12}$$

Denoting $\mathbf{x} = [\vartheta_0, \vartheta_1, \ldots, \vartheta_{\kappa-1}]^T$, $\mathbf{y} = [y_0, y_1, \ldots, y_{\kappa-1}]^T$, $\mathbf{n} = [n_0, n_1, \ldots, n_{\kappa-1}]^T$, we can obtain the following:

$$\mathbf{y} = \mathbf{H}\mathbf{x} + \mathbf{n} \tag{13}$$

where the effective channel matrix is given by

$$\mathbf{H} = \begin{bmatrix} h(0) & h(-\tau) & \cdots & h(-(\kappa-1)\tau) \\ h(\tau) & h(0) & \cdots & h(-(\kappa-2)\tau) \\ \vdots & \vdots & \ddots & \vdots \\ h((\kappa-1)\tau) & h((\kappa-2)\tau) & \cdots & h(0) \end{bmatrix} \tag{14}$$

.

REFERENCES

[1] M. Winkler, "Chirp signals for communications," in *Proc. IEEE WESCON*, 1962.

[2] A. Springer, M. Huemer, L. Reindl, C. C. W. Ruppel, A. Pohl, F. Seifert, W. Gugler, and R. Weigel, "A robust ultra-broad-band wireless communication system using SAW chirped delay lines," *IEEE Trans. Microw. Theory Techn.*, vol. 46, no. 12, pp. 2213–2219, Dec. 1998.

[3] A. Springer, W. Gugler, M. Huemer, R. Koller, and R. Weigel, "A wireless spread-spectrum communication system using saw chirped delay lines," *IEEE Trans. Microw. Theory Techn.*, vol. 49, no. 4, pp. 754–760, Apr. 2001.

[4] T. Yoon, S. Ahn, S. Y. Kim, and S. Yoon, "Performance analysis of an overlap-based CSS system," in *Proc. IEEE ICACT*, vol. 1, 2008, pp. 424–426.

[5] X. Ouyang and J. Zhao, "Orthogonal chirp division multiplexing," *IEEE Trans. Commun.*, vol. 64, no. 9, pp. 3946–3957, Sep. 2016.

[6] L. Zheng, M. Lops, Y. C. Eldar, and X. Wang, "Radar and communication coexistence: An overview: A review of recent methods," *IEEE Signal Process. Mag.*, vol. 36, no. 5, pp. 85–99, 2019.

[7] F. Liu, L. Zhou, C. Masouros, A. Li, W. Luo, and A. Petropulu, "Toward dual-functional radar-communication systems: Optimal waveform design," *IEEE Trans. Signal Process.*, vol. 66, no. 16, pp. 4264–4279, 2018.

[8] C. De Lima, D. Belot, R. Berkvens, A. Bourdoux, D. Dardari, M. Guillaud, M. Isomursu, E.-S. Lohan, Y. Miao, A. N. Barreto, M. R. K. Aziz, J. Saloranta, T. Sanguanpuak, H. Sarieddeen, G. Seco-Granados, J. Suutala, T. Svensson, M. Valkama, B. Van Liempd, and H. Wymeersch, "Convergent communication, sensing and localization in 6G systems: An overview of technologies, opportunities and challenges," *IEEE Access*, vol. 9, pp. 26 902–26 925, 2021.

[9] S. Dwivedi, A. N. Barreto, P. Sen, and G. Fettweis, "Target detection in joint frequency modulated continuous wave (FMCW) radar-communication system," in *Proc. IEEE ISWCS,*, Oulu, Finland, Aug. 2019, pp. 277–282.

[10] X. Ouyang, O. A. Dobre, Y. L. Guan, and J. Zhao, "Chirp spread spectrum toward the Nyquist signaling rate- orthogonality condition and applications," *IEEE Signal Process. Lett.*, vol. 24, no. 10, pp. 1488–1492, Oct. 2017.

[11] T. M. Pham, A. N. Barreto, and G. P. Fettweis, "Efficient communications for overlapped chirp-based systems," *IEEE Wireless Commun. Lett.*, vol. 9, no. 12, pp. 2202–2206, Dec. 2020.

[12] A. Paulraj, R. Nabar, and D. Gore,, *Introduction to space-time wireless communications*. Cambridge University Press, 2008.

[13] P. W. Wolniansky, G. J. Foschini, G. D. Golden, and R. A. Valenzuela, "V-BLAST: an architecture for realizing very high data rates over the rich-scattering wireless channel," in *Proc. IEEE ISSSE,* Pisa, Italy, Oct. 1998.

[14] L. G. Barbero, and J. S. Thompson, "A fixed-complexity MIMO detector based on the complex sphere decoder," in *Proc. IEEE SPAWC,* Cannes, France, Jul. 2006.

[15] L. G. Barbero, and J. S. Thompson, "Fixing the complexity of the sphere decoder for MIMO detection," *IEEE Trans. Wireless Commun.*, vol. 7, no. 6, pp. 2131–2142, Jun. 2008.

[16] 3GPP, "Technical report: Study on channel model for frequencies from 0.5 to 100 GHz,"Tech. Rep. 38.901, Jun. 2018, version 15.0.0.

[17] HermesPy, 2021. [Online]. Available: https://github.com/Barkhausen-Institut/hermespy